J Mater Sci (2006) 41:5820–5827
DOI 10.1007/s10853-006-0340-0

# Crystallization behavior of PZT film prepared by sol–gel route

**F. Yang · L. Wang · F. Zheng · W. D. Fei**

Received: 15 April 2005 / Accepted: 29 September 2005 / Published online: 29 June 2006


**Abstract** The X-ray scattering measurements were used to investigate $Pb(Zr,Ti)O_3$ films prepared by sol–gel process. From analysis of specular and off-specular X-ray reflectivities, the morphology of nanoscale pores in $Pb(Zr,Ti)O_3$ film was determined by adjusting a model to the observed data. It is found that nanoscale pores in the films were closely attributed to the precursor with higher molar concentration. Furthermore, nanoscale pores present a certain degree of order in the direction normal to the film surface, which mainly distribute near the interface between films and substrate. The pores gradually close with annealing time increasing, and the closing process of the pores leads to pit formation in the film surface.

## Introduction

Ferroelectric films, in particular, lead–zirconate–titante ($Pb(Zr,Ti)O_3$, PZT) films, have shown very promising properties for several applications such as non-volatile memory elements, uncooled infrared pyroelectric sensors, surface acoustic wave devices and actuators [1–3]. For ferroelectrics random access memory (FeRAM) based on PZT films, a large remnant polarization ($P_r$) is an important concern, and degradation of reversible polarization (so-called ''fatigue'') is other key parameter for device design. In addition to compositional and microstructure factors (such as Zr/Ti ratio, grain size, crystalline orientation, etc.) which dominate the properties of PZT films, the influences of internal stress, the substrate, surfaces and interfaces also have to be considered in understanding the microstructure-property relationships in the films.

Besides sol–gel technique, several approaches such as metal organic chemical vapor deposition (MOCVD), radio frequency (rf) magnetron sputtering and pulsed laser depositions (PLD) have been adopted to fabricate PZT ferroelectric films. Compared with these methods, sol–gel process has merits in compositional uniformity, easy control of doping and low cost. Many researchers have reported the high-quality films with attractive ferroelectric properties based on the sol–gel process. Up to the remnant polarization of 89.2 $\mu C/cm^2$ and 90 $\mu C/cm^2$ in Nb-doped PZT films and rare earth element-doped BLT films were well prepared by the approach [4, 5].

In many cases, such as rf-sputtering and sol–gel process, the nanoscale pores have great probability to remain in the remnant films, which results in lower density of films compared with that of bulk materials. Microstructure or interfacial structure of thin films are usually investigated by local probes, such as, scanning electron microscope (SEM), atomic force microscope (AFM) and transmission electron microscope (TEM), however, the foregoing observation routes could not give access to much better statistics information about these pores due to the difficulty on specimen

F. Yang · L. Wang · W. D. Fei (✉)
School of Materials Science and Engineering,
Harbin institute of Technology, P.O. Box 405,
Harbin 150001, P. R. China
e-mail: wdfei@hit.edu.cn

F. Zheng
Department of Applied Physics, Harbin Institute
of Technology, Harbin 150001, P. R. China

preparation and probe limitation. X-ray reflectivity (XRR) and X-ray diffuse scattering measurements are non-destructive tools well suited to investigate thin layers [6–8], which can provide information on the electronic density profile in depth, interfacial or surface structure, and the size of inclusion in the matrix. There have been many works about the effect of the microstructure on the dielectric properties of PZT films; however, few efforts have been paid to reveal the arrangement of the nanoscale pores in the films.

In the article, research interest is to investigate the morphology of nanoscale pores in PZT film prepared by sol–gel process, and the evolution of pores as a function of process conditions is also discussed.

## Experimental

The $Pb(Zr_{0.52}Zr_{0.48})O_3$ films were prepared by a modified sol–gel process. Lead acetate trihydrate, zirconium oxynitrate, and titanium *n*-butoxide were used as the starting materials; 1-methoxyethanol and acetyacetone were used as solvent and chelating agent, respectively. 10 mol% Pb excess was added to compensate the PbO volatilized during annealing. Lead acetate trihydrate and zirconium oxynitrate were initially dissolved in 1-methoxyethanol, and solution was heated up for 1 h at 100 °C. During the process, the acetyacetone was added to stabilize the solution. Then, the required quantity of titanium *n*-butoxide was dropped, and the resultant solution was refluxed at 124° C till a transparent precursor was obtained. In the present work, the precursors with the molar concentration of 0.3 mol/l and 0.5 mol/l were synthesized to prepare the PZT films; for simplified representation, the precursor with the molar concentration of 0.3 mol/l is abbreviated as P3, the other precursor as P5.

The wet film was prepared by spinning the solution on $Pt(111)/Ti/SiO_2/Si(001)$ at 6,000 rev/min for 20 s, dried at 120 °C for 10 min, then given a pyrolysis treatment at 350 °C for 10 min, and the remnant film was obtained by repeating the above process for 4 times. Finally, PZT films were annealed at 600 °C for different intervals (15, 30, 45 and 60 min) by conventional thermal annealing.

The microstructures of the PZT films prepared with P5 and P3 precursors were investigated on a Hitachi S-3000N type scanning electron microscope (SEM), and the crystal structure and orientation of the films were analyzed on a Philips X′ pert type X-ray diffractometer. Small angle X-ray scattering (SAXS) technique is employed to characterize the morphology of pores in PZT films.

## Results and discussion

### Crystal structure analysis of PZT films

Figure 1 presents the typical X-ray diffraction patterns of PZT films prepared with different precursors, and the thickness of the films was characterized by cross-sectional SEM, which give values of 700 nm and 400 nm for PZT films prepared with P5 and P3 precursor, respectively, as displayed in Fig. 2, moreover, the latter is consistent with the simulation results of X-ray reflectivity. XRD results show that the PZT films were single perovskite phase and well crystallized after annealing at 600° C for 30 min or longer, however, it should be figured out that there is somewhat difference in the crystalline orientation of two PZT films. The PZT film prepared with P5 precursor are slightly 111-oriented, since there is considerable (110) diffraction; while for the film prepared with P3 precursor, 110-diffraction is hardly been observed, as shown in Fig. 1 (b), and intensity of 111-diffraction of PZT films evidently exceeds that of 100-diffraction, which suggests the 111-oriented crystalline structure in the film. Two key factors may contribute to the difference in the (111)-preferred orientation between the films prepared by two precursors: First, the different film thickness between two films. As film thickness increases (400 nm to 700 nm), the effect of (111)-preferred nucleation on (111)-oriented Pt substrate plays less dominated role in the (111)-preferred growth, and there is more possibility of randomly oriented nucleus form in thicker films, which makes the orientation diffusive; Second, it may result from the discrepancy of solid clusters size in precursors with different molar concentration. It has

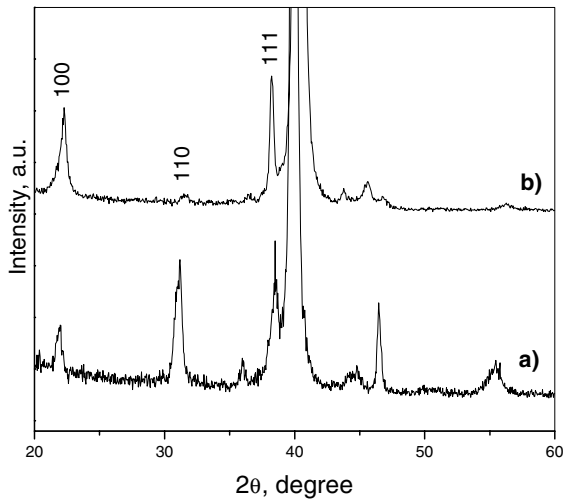


**Fig. 1** XRD patterns of PZT films annealed at 600 °C for 30 min. (**a**) prepared with P5 precursor; (**b**) prepared with P3 precursor

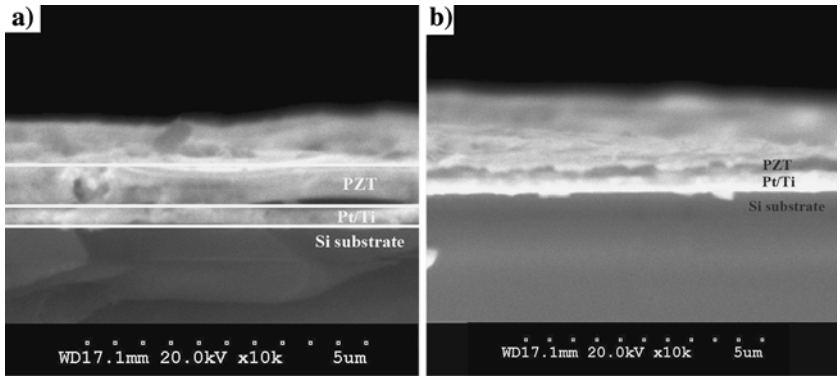


**Fig. 2** Cross-sectional morphology of PZT films annealed at 600 °C for 30 min. (**a**) prepared with P5 precursor; (**b**) prepared with P3 precursor

been noted that particles in PZT precursor solutions are chain-like and have a direct effect on the orientation of the thin films and the pyrochlore to perovskite phase transformation properties. The precursor with bigger solid clusters unusually leads to 111-oriented growth. In the case of sol–gel processing with identical starting materials, more possibility in aggregation of particles accounts for bigger colloidal particles of higher molar concentration precursor than that in lower one.

To further study the effect of precursors with different molar ratios on the film texture, PZT films are investigated by an $\omega$-scan of X-ray diffraction, in which the 111-diffraction is analyzed. In the case of $\omega$-scan, $2\theta$ is fixed at that of PZT 111-diffraction and incidence angle ($\omega$) of X-ray changes continuously. The $\omega$-scan curves for 111-diffraction of two PZT films are present in Fig. 3. Gaussian distribution function can be used to simulate the dispersity of film texture because the spatial distribution of the texture axis (the normal of oriented planes) meets Gaussian distribution [9]:

$$I = I_0 + \frac{A}{w\sqrt{\pi/2}} e^{-2\frac{(\omega-\omega_c)^2}{w^2}} \quad (1)$$

where $\omega_c$ is ideal position of texture axis and $w$ represents the dispersity of film texture. $w$ can be obtained by the Gaussian simulation (using Eq. 1) of the $\omega$-scan curves, as shown in Fig. 3, and the smaller $w$ suggests the better orientation of the film. One can figure out that the PZT film prepared with P3 precursor is better 111-oriented, since it has lower $w$, which is consistent with the aforementioned results of crystal structure analysis.

## Surface morphology analysis of PZT films

The microstructures of annealed PZT films prepared with different molar concentration precursors are shown in Fig. 4. The SEM images show that the surface morphologies of the two annealed PZT films are quite different, the surface of PZT film prepared with P3 precursor is dense and crack-free, however, there are

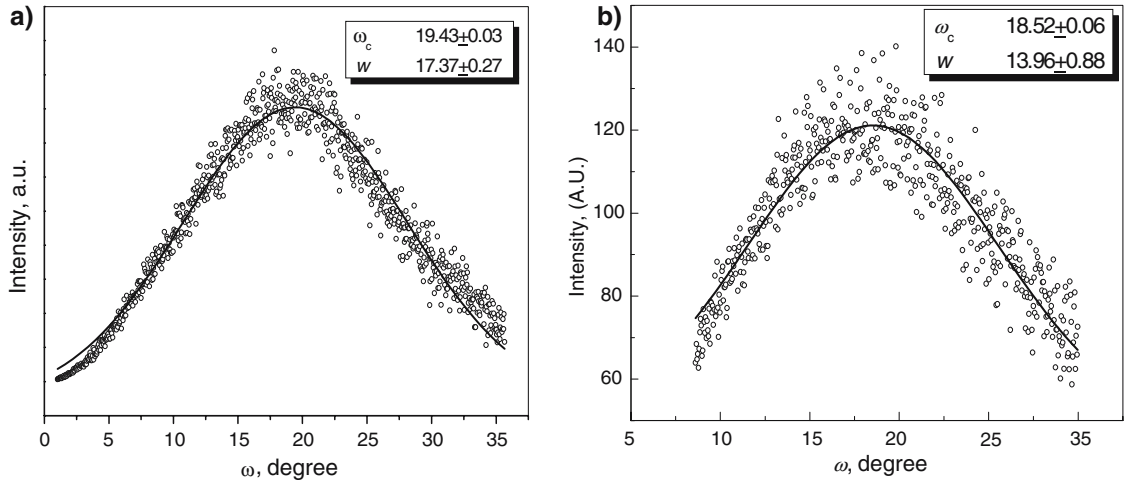


**Fig. 3** Typical experimental $\omega$-scan curves and corresponding Gaussian fits of PZT films annealed at 600° C for 30 min. (**a**) prepared with P5 precursor; (**b**) prepared with P3 precursor

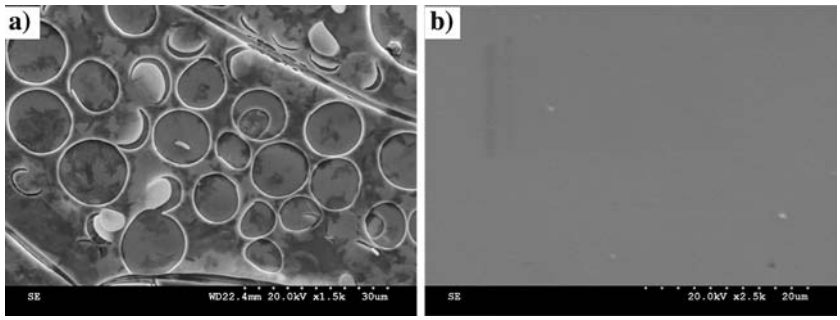


**Fig. 4** Typical surface morphologies of PZT films annealed at 600 °C for 30 min (**a**) prepared with P5 precursor; (**b**) prepared with P3 precursor

many circular pits distributing on the surface of the PZT film prepared with P5 precursor. Since the two PZT films were prepared through the same annealing process, the different surface morphologies between the PZT films indicate that the particular surface structure is straightforward relevant with the precursor. Figure 5 shows the magnitude of surface morphology of PZT films prepared with P5 precursor, which exhibits the circular substances (marked as ''A'') leaving on the surface of PZT films, one can observe that the form of the substances matches the mentioned surface pits accordingly, then it is obvious that the surface pits are the result of peel off effect of surface layer.

## X-ray scattering analysis of PZT films

SAXS technique, i.e., $\omega$-$2\theta$ scan in small angle range, which including X-ray reflection and X-ray diffuse scattering, was adopted to study the PZT films prepared with different precursors. Figure 6 is the $\omega$-$2\theta$ scan curves of X-ray scattering of PZT films. In the PZT film prepared with P5 precursor, it could be found obvious fluctuations with separation of about 2°, while no such fluctuations can be seen in the PZT film prepared with P3 precursor. The phenomenon shown in the X-ray scattering pattern of PZT film prepared with P5 precursor may not be kiessig fluctuation that characterizes the film thickness, in our case, it comes forth in lower angle, as an arrow pointing out in Fig. 6(a) for clarity (the appearance of kiessig fluctuation also indicates that the surface of PZT film is smooth with low roughness), it can be addressed that the fluctuation at higher angles in $\omega$-$2\theta$ scan curve of X-ray reflection implicates that there exists electron density fluctuation in the normal direction of the film surface. The X-ray scattering patterns of PZT films prepared with P5 precursor as a function of annealing time are also shown in Fig. 6(b), it could be found that the PZT films after different annealing times have similar fluctuation, but the intensity of fluctuation gradually decreases with prolong of the annealing time.

As shown in Fig. 1, no other phase diffraction peaks can be found except Pt and PZT, but the clear fluctuations at higher angles in $\omega$-$2\theta$ scan of X-ray reflection given in Fig. 6 suggest that the fluctuation of electron density in the film with P5 precursor is considerable, therefore, we infer that such fluctuations at high angles in $\omega$-$2\theta$ scan of X-ray arise from the existing pores in the film.

Based on the kinematical approximation, X-ray scattering intensity of $\omega$-$2\theta$ scan can be written as following:

$$I(q_z) = A^2 \left| \int_0^L \rho(z) e^{-iq_z z} dz \right|^2 \tag{2}$$

where $A$ is illuminated area of film by X-ray beam, $\rho(z)$ is the average electron density of the film at position $z$ (distance to the interface between film and substrate), $q_z$ is the component in $z$-direction ( normal direction of the film) of scattering vector and $L$ is the thickness of films. For the heterogeneous thin film, X-ray reflectivity of PZT films indicated that there is a cumulative order of distribution of pores in the direction normal to the film surface, so the total electron

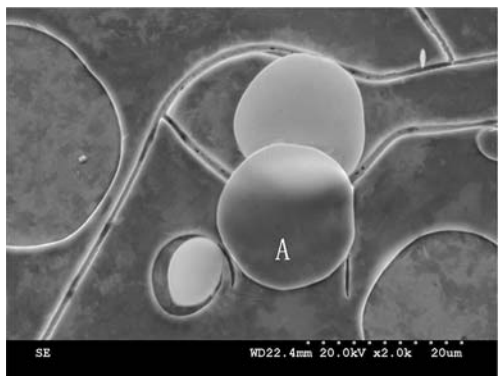


**Fig. 5** The magnitude of morphology of PZT films annealed at 600 °C for 30 min (prepared with P5 precursor)

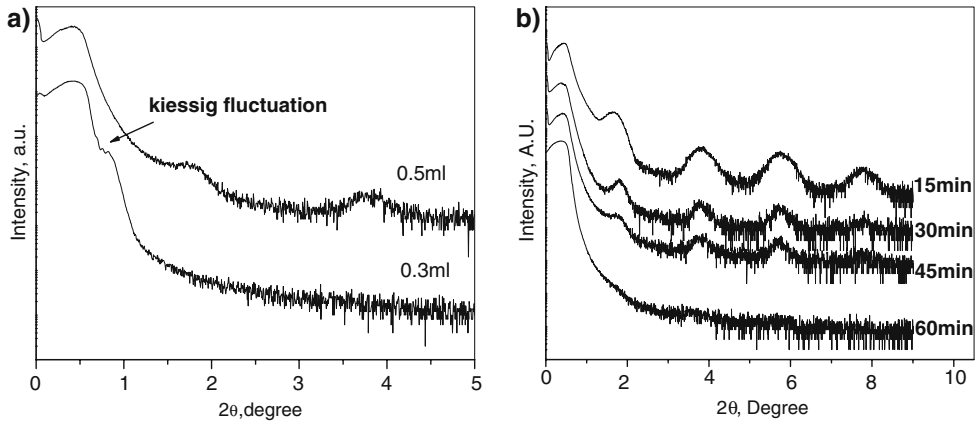


**Fig. 6** $\omega - 2\theta$ scan curves of X-ray scattering for PZT films annealed at 600 °C (**a**) effect of precursors with different molar ratios (annealed for 30 min); (**b**) effect of annealing time (prepared with P5 precursor)

density of film can be written as the sum of Gaussian functions:

$$\rho(z) = \rho_m\left(1 - \sum A_i e^{-a_i(z-z_i)^2}\right) \tag{3}$$

where, $\rho_m$ is the electron density of PZT matrix, subscript $i$ stands for the position index of pores. The scattering intensity profile at higher angles is written from Eqs. 2 and 3 as

$$I_D(q) = A^2 \int_0^L \rho(z) e^{-iqz} dz = A^2 \rho_m \int_0^L \left(1 - \sum A_i e^{-a_i(z-z_i)^2}\right) e^{-iqz} dz \tag{4}$$

in actual calculation, the vibration of $L$ must be considered accordingly due to the effect of surface or interfacial roughness. Figure 7a showed the typical simulation of X-ray reflectivity and measurement data, in which the inset curve is distribution of electron density, and the distribution of pores along the normal direction as a function of annealing interval is shown in Fig. 7b. The simulation indicated that the pores exist parallel to the interface between PZT films and Pt substrate, with the distance of about 4 nm and 8 nm to the interface. With annealing time increasing, the distance changes little.

From the above analysis and simulation, the $z$-direction profiles of pores distribution of PZT films were obtained, however, the information on characteristic size of pores is needed to completely reveal the morphology of pores in PZT films, The main obstacle to characterize the morphology of pores in thin films by X-ray scattering is that the scattering intensity of PZT films with pores in the XRR profile contains the contribution of film matrix. $\omega - 2\theta$ scan of X-ray scattering with a small offset angle deviating from reflection

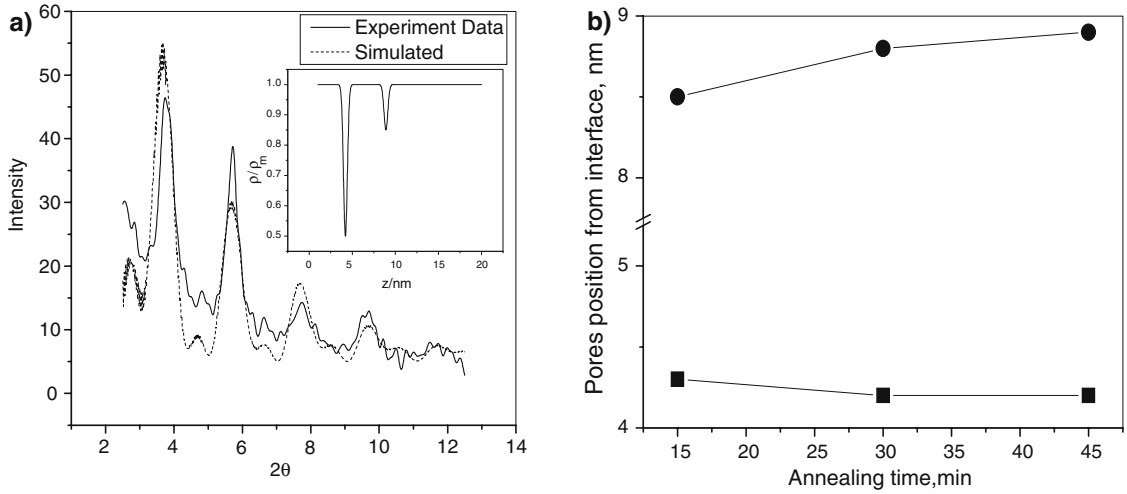


**Fig. 7** (**a**) X-ray reflectivity data and fitted curves of PZT films prepared with P5 precursor by simulation of corresponding electron density profiles in $z$ direction; (**b**) pores position from interface as a function of annealing time

geometry (abbreviated as offset $\omega - 2\theta$ scan) is a useful technique to analyze the surface and interface of the coating and thin films. In most cases, a 0.1° offset is enough to avoid the reflectivity of PZT films, so in the assumption of weak lateral correlation (or at least the exist correlation is too minute to be detected within the precision of experiment), the intensity of nanoscale pores scattering can be written as [10–12]

$$I_D(q) = I_0 \frac{[\sin(qR) - qR\cos(qR)]^2}{(qR)^6} \times \frac{1 - e^{-2q^2\sigma_d^2}}{1 - 2e^{-q^2\sigma_d^2}\cos(qd) + e^{-2q^2\sigma_d^2}} \quad (5)$$

in Eq. 5, $R$ and $d$ are gyration radius of pores and interspacing distance between neighboring pores, ?and $\sigma_d$ stands for the variance of $d$.

The typical offset $\omega - 2\theta$ scan curves of the PZT film prepared with P5 precursor are exhibited in Fig. 8. The peak positions of the latter three fluctuation humps do not shift with offset angle, which suggests that the fluctuation at higher angles may result from the pores scattering. By gradually changing the offset angle, the reflectivity will be absolutely absent at an appropriate offset angle ($\alpha_i$). Then the offset $\omega - 2\theta$ scan curve of annealed PZT films at the offset $\alpha_i$ angle can give the information on the gyration radius and interspacing distance of pores. It is interesting to comment that the first fluctuation hump, as arrows pointing for clarity, moves orderly with offset angle, indicating some order structure on the surface.

It should be noted that the $\boldsymbol{q}$ direction of offset $\omega - 2\theta$ scan is nearly parallel to the film normal direction, considering that the angle between $\boldsymbol{q}$ and film normal direction equals the offset angle (≈0.2°),

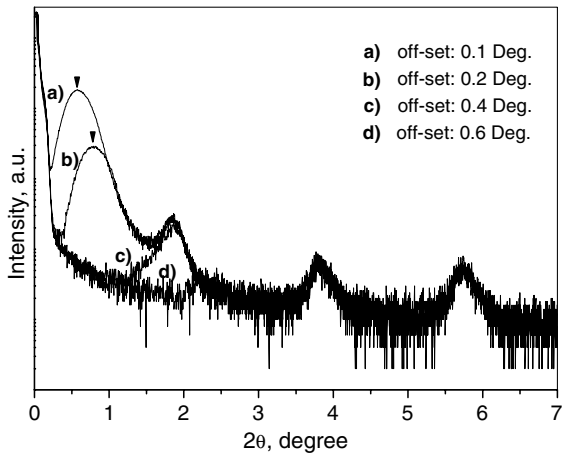


**Fig. 8** Typical offset $\omega - 2\theta$ scan curves of PZT film annealed at 600 °C for 30 min (prepared with P5 precursor)

and the $\boldsymbol{q}$ direction does not change during offset $\omega - 2\theta$ scan measurement, therefore, Eq. 5 can be used here, although it is for the spherical like inclusion analysis. In this case, $R$ in Eq. 5 represents the gyration radius of pores along $z$-direction, while $d$ is the interspacing distance among pores. The corresponding $z$-directional radius and interspacing distance among pores in PZT films could be attained by simulation using Eq. 5, as shown in Fig. 9(a), the effect of annealing time on the pores is also exhibited in Fig. 9(b). The gyration radius of pores along $z$-direction is 0.5 nm in PZT film annealed for 15 min, with annealing time increases, the radius gradually decreases, and after annealing for 60 min, the pores in PZT films completely close up. The conclusion is consistent with the result of $\omega - 2\theta$ scan curve of the PZT film annealed for 60 min, which indicates that the fluctuation resulting from the pores disappears.

## Discussion

From above analysis, one can conclude that PZT film prepared with P5 precursor exhibits the particular surface morphology with circular pits, and SAXS study results of the film indicate that there are nanoscale pores with a certain degree order in the $z$-direction near the interface between PZT films and Pt substrate in the films. Furthermore, it is worthy to point out that the surface circular pits appear along with the emergence of inside pores near the interface, and PZT films without surface pits exhibit no inside pores morphology, as in the case of films prepared with P3 precursor. It would be suggested that the surface pits were closely related to the pores evolution in PZT films, and the pores evolution is associated with the precursor, so we prostitute a mechanism of evolution of surface pits and inside pores in the PZT films, as shown in Fig. 10, which relates evolution of surface pits and pores to the residual stress in the films.

As it has been mentioned, for PZT films prepared by sol–gel process, organic decomposing in the pyrolysis treatment and the volume shrinkage during ferroelectric transition lead pores engender in the films. In general, porosity of the films increases during pyrolysis process, and the crystallization process of the films by annealing at elevated temperature makes pores closing to reduce the surface energy. X-ray scattering analysis indicated that the closing rates of pores in the films prepared with the higher molar concentration precursor would be much less than that of films prepared with lower molar concentration precursor, it needs longer annealing time (60 min) for complete closing of pores in the films prepared with P5 precursor. On the other

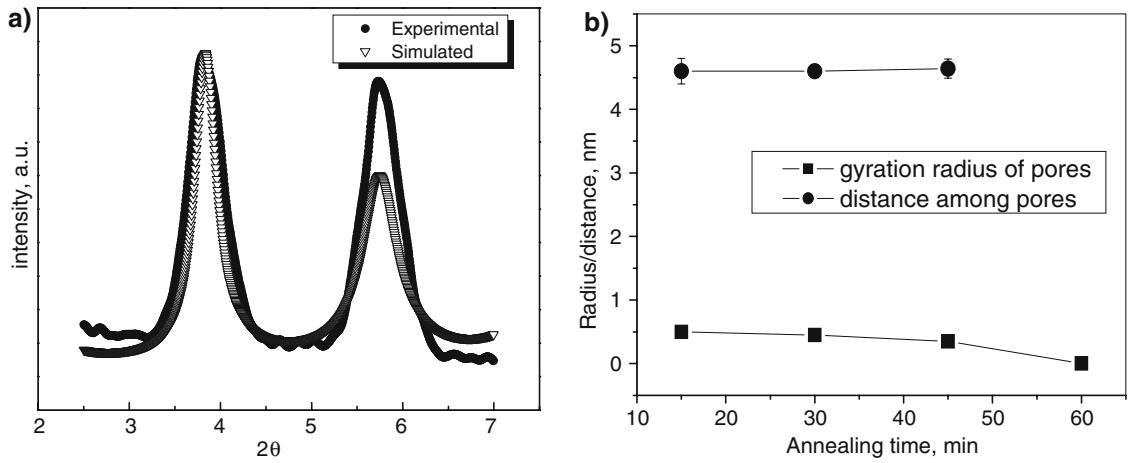


**Fig. 9** (**a**) offset $\omega - 2\theta$ scan curve of X-ray for PZT films and fitted curves of PZT films annealed at 600 °C for 30 min; (**b**) gyration radius of pores along $z$-direction and corresponding interspacing distance among pores as a function of annealing time

hand, residual stress should be taken into account to reveal the origin of the surface pits in the films surface, since it would have a great effect on the evolution of inside pores of films. Due to the cubic-tetragonal transition and the effect of substrate constraint, there exists considerable residual stress in the polycrystalline PZT films when cooling down for 600 °C to room temperature. The previous study showed that there are tensile stresses in the PZT films prepared with P5 precursor, in this case the tensile stress will be the main obstacle of closing process of pores in the $x - y$ plane (film surface plane), furthermore, clamping effect of substrates is more remarkable near the interface between films and Pt substrate, then the pores may have maximum possibility of leaving near the interface. Otherwise, the two-dimensional stress has less restrictive effect on the closing of pores along $z$-direction than that in $x - y$ plane, and normal tensile stress will be induced by the closing process of the pores along $z$-direction near interface. On the combined effect of the residual tensile stress and the normal tensile stress, the local area of PZT film would peel off from the corresponding location on the surface layer, leading to many resultant pits in film surface. From the SEM image and simulation of $\omega - 2\theta$ scan of PZT films, the pores near interface would be disc-like shape, with $z$-directional gyration radius of 0.5 nm and analogic lateral size compared with surface pits.

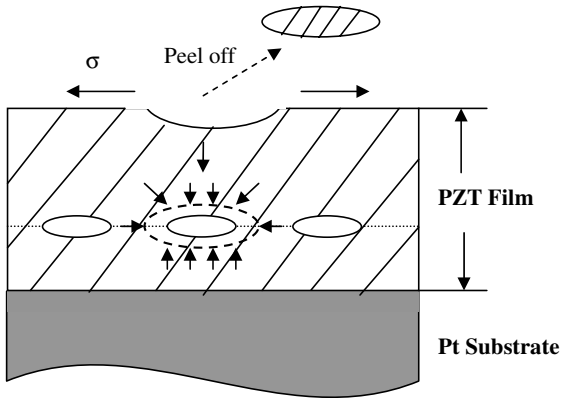


**Fig. 10** Schematic mechanism of the evolution of surface structure and inside pores in PZT films prepared with P5 precursor

## Conclusions

The crystallization process of PZT films prepared by sol–gel route was investigated by X-ray scattering measurements. The main results were obtained as follows:

(1) The PZT films prepared by sol–gel process were crystallized by annealing at 600 °C, and PZT films prepared with P5 and P3 precursors were both 111-oriented, while the former film has better orientation.
(2) The appearance of nanoscale pores in PZT films was related to the higher molar concentration precursor, furthermore, nanoscale pores in the films present a certain degree of order in the direction normal to the surface of the films, which mainly distribute near the interface between films and substrate.
(3) The average radius of pores along $z$-direction is about 0.5 nm before films crystallization, which continues to reduce after longer annealing, along with appearance of pits in the film surface.

## References


1. Pintilie L, Pereira M, Gomes MJM, Boerasu L (2004) Sensors Actuator A 115:185
2. Souza ECF, Simöes AZ, Cilense M, Longo E, Varela JA (2004) Mater Chem Phy 88:155
3. Du H, Johnson DW, Zhu W, Graebner JE, Kammlott GW, Jin S, Rogers J, Willett R, Fleming RM (1999) J Appl Phys 86:2220
4. Chon U, Jang HM, Kim MG, Chang CH (2002) Phys Rev Lett 89:087601
5. Han H, Song XY, Zhong J, Kotru S, Padmini P, Dandey RK (2004) Appl Phys Lett 85:5310
6. Chamard V, Dolino G, Stettner J (2000) Physica B 283:135
7. Buttard D, Dolino G, Bellet D, Baumbach T, Rieutord F (1999) Solid State Com 109:1
8. Lopez JM, Navarro M, Papadimiriou D, Bassas J, Samitier J (1996) Thin Solid films 276:238
9. Yang F, Zheng F, Fei WD (2005) Key Eng Mater 280–283:857
10. Hazra S, Gibaud A, Sella C (2004) Appl Phys Lett 85:395
11. Gibaud A, Sella C, Maaza M, Sung L, Dura JA, Satija SK (1999) Thin Solid Films 340:153
12. Hazra S, Gibaud A, Désert A, Sella C, Naudon A (2000) Physica B 283:97